MRS Advances © 2018 Materials Research Society
DOI: 10.1557/adv.2018.373

New Methods for the Fabrication of Composites for Supercapacitor Electrodes with High Active Mass Loading

Aseeb M. Syed and Igor Zhitomirsky

Department of Materials Science and Engineering, McMaster University

ABSTRACT

MnO_2-multiwalled carbon nanotube (MWCNT) supercapacitor electrodes with active mass loading of 30-45 mg cm^{-2} were prepared. In method 1, MnO_2 and MWCNT were dispersed using 3,4-dihydroxybenzaldehyde (DHB) and toluidine blue (TD), respectively. The Schiff base formation between amino group of TD and aldehyde group of DHB facilitated improved mixing of MnO_2 and MWCNT. In method 2, gallocyanine (GC) was used as a co-dispersant for MnO_2 and MWCNT. The catecholate type bonding of DHB and GC allowed for adsorption of the dispersant molecules on MnO_2 nanoparticles. The electrodes, prepared by method 1 showed higher capacitance, compared to the electrode, prepared by method 2. The highest capacitance of 7.8 F cm^{-2} (173 F g^{-1}, 139 F cm^{-3}) was obtained at a scan rate of 2 mV s^{-1} and active mass loading of 45 mg cm^{-2}.

INTRODUCTION

MnO_2 is currently under intensive investigation for energy storage applications in electrodes of supercapacitors (SC)[1-4]. The interest in application of MnO_2 in SC electrodes is due to high theoretical capacitance of this material, nearly ideal capacitive charge-discharge behavior in a relatively large voltage window and low cost. MnO_2 is usually combined with conductive additives in order achieve enhanced electronic conductivity of composites.

MnO_2 and composite electrodes showed [5-9] high gravimetric capacitances (C_m, F g^{-1}) at low active mass loadings in the range of 0.005–1 mg cm^{-2}. However, significantly higher active mass loadings above 10 mg cm^{-2} are necessary for practical applications[10,11]. It was found that C_m decreased drastically with increasing active mass due to poor electrolyte access to the active material and low electronic conductivity. Areal capacitance (C_S, F cm^{-2}) is another important parameter of SC, especially at high active mass loadings. The important task is to achieve good performance at high active mass loadings[11] and fabricate SC electrodes with high C_S and C_m.

The goal of this investigation was the development of colloidal strategies for the fabrication of MnO_2-MWCNT electrodes with mass loadings in the range of 30-45 mg cm^{-2}. The approach was based on the use of advanced dispersants for dispersion and mixing of MnO_2 and MWCNT, which facilitated the fabrication of efficient SC electrodes with high C_S and C_m.

EXPERIMENTAL SECTION

Toluidine blue (TD), 3,4-dihydroxybenzaldehyde (DHB), gallocyanine (GC), polyvinyl butyral (PVB), $KMnO_4$, Na_2SO_4 (Aldrich, Canada), MWCNT (ID 4 nm, OD 13 nm, length 1-2 um, Bayer, Germany) and Ni foams (95 % porosity, Vale, Canada) were used. MnO_2 particles were obtained by reduction of Mn^{7+} species in aqueous $KMnO_4$ solutions using ethanol as a reducing agent. Two methods were developed for the preparation of MnO_2-MWCNT electrodes. In method 1, MnO_2 and MWCNT were dispersed using DHB and TD, respectively. The individual suspensions of MWCNT and MnO_2 were mixed. In method 2, MnO_2 and MWCNT were mixed and dispersed using GC as a co-dispersant. The mass ratio MnO_2:MWCNT was 4:1. PVB binder was dissolved in ethanol and added to composite MnO_2:MWCNT material, which was then impregnated in Ni foam current collectors. The binder content in the electrodes was 3%. The impregnated foams were pressed in order to reduce contact resistance.
TEM studies were performed using a FEI Tecnai Osiris microscope. X-ray diffraction (XRD) experiments were carried out using a Nicolet I2 powder diffractometer with monochromatized CuKα radiation. Cyclic voltammetry (CV) and impedance spectroscopy investigations were performed using a potentiostat (PARSTAT 2273, Princeton Applied Research, USA). The capacitive behavior of the electrodes was studied in three-electrode cells using 0.5 M Na_2SO_4 aqueous solutions. The area of the working electrode was 1 cm^2. The counter electrode was a platinum gauze, and the reference electrode was a saturated calomel electrode (SCE). CV studies were performed at scan rates of 2-100 mV s^{-1}. The areal capacitance $C_S=Q/\Delta VS$ and gravimetric capacitance $C_m=Q/\Delta Vm$ were calculated using half the integrated area of the CV curve to obtain the charge Q, and subsequently dividing the charge Q by the width of the potential window ΔV and electrode area S or mass loading m. The alternating current measurements of complex impedance $Z^*=Z'-iZ''$ were performed in the frequency range of 10 mHz - 100 kHz at a signal amplitude of 5 mV. The complex differential capacitance $C_S^*=C_S'-iC_S''$ was calculated[12] from the impedance data as $C_S'=Z''/\omega|Z|^2S$ and $C_S''=Z'/\omega|Z|^2S$, where $\omega=2\pi f$ (f-frequency).

RESULTS AND DISCUSSION

Fig.1 shows TEM and XRD data for MnO_2. The size of the particles was 30-50 nm (Fig.1(A)). The XRD studies revealed small peaks of a birnessite MnO_2 phase. The XRD peak broadening (Fig.1(B)) resulted from the small particle size. However, the samples also contained an amorphous phase.
Fig 2(A-C) shows chemical structures of TD, DHB and GC used in this investigation for the surface modification and dispersion of MWCNT and MnO_2. MWCNT were dispersed using TD and GC dyes as dispersants. Recent studies[13] showed that various organic dyes allow for non-covalent functionalization and efficient dispersion of MWCNT. The non-covalent functionalization[13] offers advantages for MWCNT applications, based on high electronic conductivity of MWCNT. The small size of charged organic dyes facilitated MWCNT dispersion via the “unzipping” mechanism[13]. This mechanism involved gap formation at the MWCNT bundle ends in suspensions during ultrasonication. The diffusion of charged dyes along the open space between the individual MWCNT, dye adsorption on MWCNT and electrostatic repulsion facilitated separation and dispersion of the individual MWCNT[13]. It is suggested that the polyaromatic structure (Fig.2) of TD and GC facilitated adsorption of the dyes on MWCNT. The adsorption mechanism of TD and GC on MWCNT involved π-π

interactions. The positive charge of adsorbed TD and GC facilitated electrostatic dispersion of MWCNT.

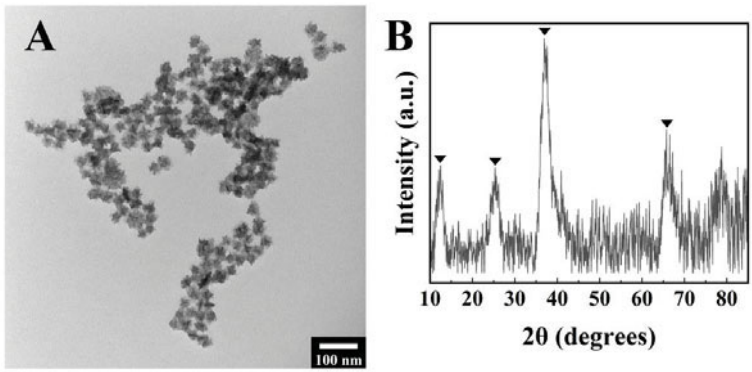

Fig.1 (A) TEM image and (B) X-ray diffraction pattern of MnO_2 (▼-JCPDS 87-1497)

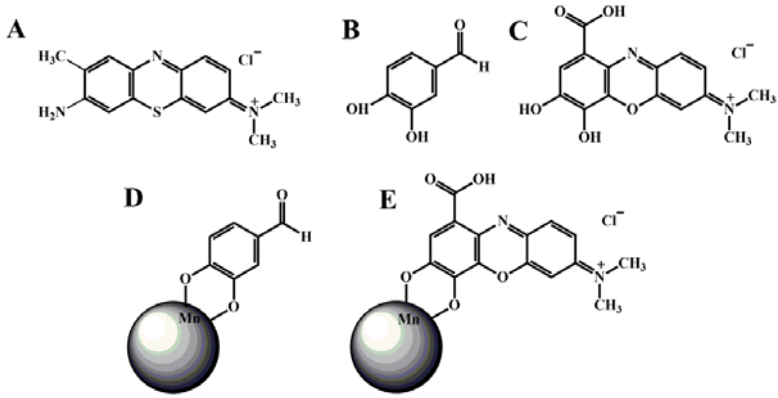

Fig.2 Chemical structures of (A) TD, (B) DHB (C) GC, (D) DHB adsorption on MnO_2, (E) GC adsorption on MnO_2.

DHB and GC belong to the catechol family of molecules (Fig.2(B,C)). Catecholates[14] showed strong adsorption on various inorganic materials and allowed efficient dispersion of inorganic nanoparticles. The catecholate adsorption[14] mechanism is based on bonding of deprotonated OH groups of catechol to metal atoms on the particle surface. Such mechanism (Fig.2(D,E)) can be suggested for the DHB and GC adsorption on MnO_2. We suggested that Schiff base[15,16] formation between amino groups of TD and aldehyde groups of DHB resulted in linking of MnO_2 and MWCNT and allowed their

improved mixing in method 1. The use of GC as a co-dispersant for MnO_2 and MWCNT facilitated improved dispersion and mixing of MnO_2 and MWCNT in method 2.

The MnO_2-MWCNT composites, prepared by methods 1 and 2 were used for the electrochemical testing. Fig.3 compares capacitive behavior of the electrodes with mass loading of 30 mg cm^{-2}, prepared using methods 1 and 2. Cyclic voltammetry (CV) studies of the electrodes (Fig.3(A)) showed nearly ideal box shapes of CVs, which indicated that good capacitive behavior was achieved at high active mass loadings. The electrodes, prepared by method 1 showed larger CV areas, which were attributed to higher capacitance. The capacitances were calculated from the CV data at different scan rates and presented in Fig.3(B). The electrodes, prepared by method 1 showed higher capacitances in the scan rate range of 2-100 mV s^{-1}. The highest capacitance of 4.2 F cm^{-2} was obtained at a scan rate of 2 mV s^{-1}.

The capacitance decreased with increasing scan rate due to diffusion limitations of electrolyte in the electrode. It is suggested that method 1 allowed improved mixing of MnO_2 and MWCNT, which resulted in higher capacitance. Therefore, the MnO_2-MWCNT composites, prepared by method 1 were investigated for the fabrication of electrodes with higher mass loadings in the range of 35-45 mg cm^{-2}.

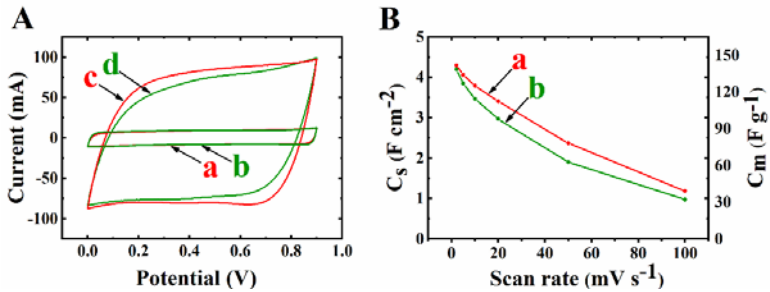

Fig.3 (A) CVs at scan rates of (a,b) 2 and (c,d) 20 mV s^{-1} for electrodes, prepared using (a,c) method 1 and (b,d) method 2, (B) C_S and C_m for electrodes, prepared using (a) method 1 and (b) method 2 for mass loading of 30 mg cm^{-2}.

The electrodes, prepared by method 1 showed good capacitive behavior at mass loadings as high as 35-45 mg cm^{-2}. Fig.4(A) shows CVs at scan rates of 2 and 20 mV s^{-1} for MnO_2-MWCNT electrode with active mass loading of 45 mg cm^{-2}. The CVs were of nearly ideal box shape. Fig.4(B,C) shows C_S and C_m data for electrodes with mass loadings of 35, 40 and 45 mg cm^{-2}, prepared by method 1. The increase in the mass loadings resulted in increased C_S at low scan rates. The analysis of C_S and C_m at different scan rates showed significant reduction of capacitance with increasing scan rate. The highest capacitance of 7.8 F cm^{-2} (173 F g^{-1}, 139 F cm^{-3}) was obtained at a scan rate of 2 mV s^{-1} and mass loading of 45 mg cm^{-2}. The analysis of impedance data for the electrodes with active mass loadings of 30 mg cm^{-2}, prepared by methods 1 and 2, showed relatively low resistance R=Z' (Fig.5(A)), which is beneficial for supercapacitor applications. The slopes of the curves in the Nyquist plots were close to the 90º and indicated good capacitive behavior. The components of complex differential capacitance have been calculated from the impedance data and presented in Fig.5 (B,C).

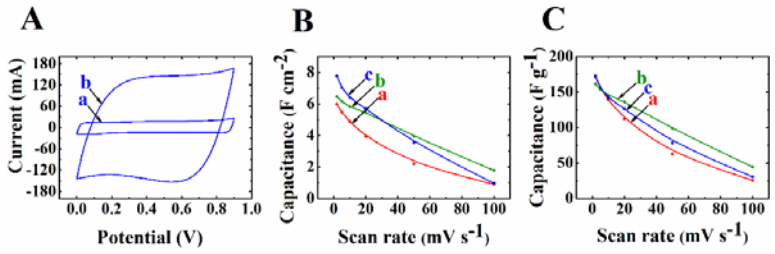

Fig.4 (A) CVs at scan rates of (a) 2 and (b) 20 mV s^{-1} for electrodes prepared by method 1 and mass loading of 45 mg cm^{-2}, (B,C) dependences of (B) C_S and (C) C_m on scan rate for electrodes with mass loadings of (a) 35, (b) 40 and (c) 45 mg cm^{-2} and thickness of (a) 0.44, (b) 0.50 and (c) 0.56 mm, prepared by method 1.

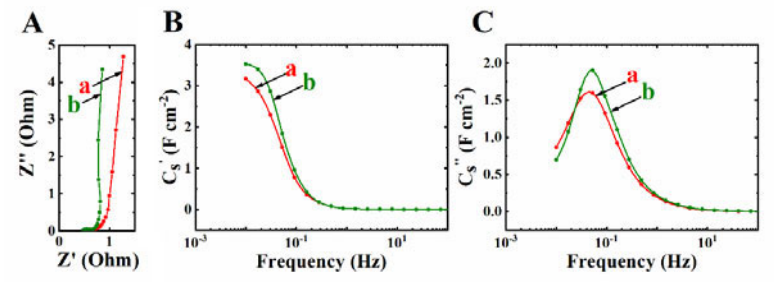

Fig.5 (A) Nyquist plots of complex impedance, (B) C_S' and (C) C_S'' versus frequency for electrodes prepared by (a) method 1 and (b) method 2 for mass loading of 30 mg cm^{-2}.

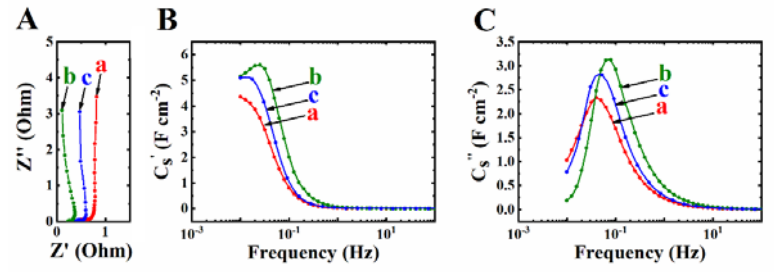

Fig.6 (A) Nyquist plots of complex impedance, (B) C_S' and (C) C_S'' versus frequency for electrodes prepared by method 1 and mass loadings of (a) 35, (b) 40 and (c) 45 mg cm^{-2}.

The frequency dependences of the capacitance showed a relaxation type dispersion [12], as indicated by the decrease in the real part of capacitance C_S' with frequency and corresponding relaxation maxima in the frequency dependences of the imaginary part C_S''. The Nyquist plots for complex impedance for mass loadings of 35-45 mg cm^{-2} were

close to the 90º and relatively low resistance R=Z' was obtained (Fig.6(A)). The frequency dependences of the components of complex capacitance showed a relaxation type dispersion (Fig.6(B,C)). The increase in mass loading from 30 to 45 mg cm^{-2} did not result in significant reduction in relaxation frequency. Therefore, the results of the analysis of impedance data, coupled with CV data indicated that good electrochemical performance was achieved at mass loadings of 30-45 mg cm^{-2}. It is important to note that the integral capacitance, calculated from the CV data in the voltage window of 0.9 V depended on scan rate, whereas differential capacitance C_S', measured using an AC signal with amplitude of 5 mV, depended on frequency. However, the comparison of C_S and C_S', measured at the same time scale, showed that C_S values were typically higher than C_S'. The difference in the differential and integral capacitances can be attributed to various factors discussed in the literature[17-19], such as poor access of ions to redox sites at low voltages, physical heterogeneity of the electrodes and other factors. The capacitance C_S of MnO_2-MWCNT electrodes, obtained using method 1, was higher, compared to the capacitance of MnO_2-MWCNT electrodes prepared by other methods [20,21] at high active mass loadings.

CONCLUSIONS

MnO_2-MWCNT electrodes with mass loadings of 30-45 mg cm^{-2} were prepared for application in SC. In method 1, MnO_2 and MWCNT were dispersed using DHB and TD, respectively. The Schiff base formation between amino group of TD and aldehyde group of DHB facilitated improved mixing of MnO_2 and MWCNT. In method 2, GC was used as a co-dispersant for MnO_2 and MWCNT. The catecholate type bonding of DHB and GC facilitated strong adsorption of the dispersant molecules on MnO_2 nanoparticles. The electrodes, prepared by method 1 showed higher capacitance, compared to the electrode, prepared by method 2. The highest capacitance of 7.8 F cm^{-2} (173 F g^{-1}, 139 F cm^{-3}) was obtained at a scan rate of 2 mV s^{-1} and active mass loading of 45 mg cm^{-2}. The high capacitance was achieved at low electrode resistance. The electrodes, prepared by method 1 are promising for SC applications.

References

[1] T. Brousse, P.L. Taberna, O. Crosnier, R. Dugas, P. Guillemet, Y.Scudeller, Y.Zhou, F. Favier, D. Belanger, and P. Simon, J. Power Sources, 173, 633 (2007)
[2] F. Grote, R.S..Kuhnel, A. Balducci, and Y. Lei, Appl. Phys. Lett., 104, 053904 (2014).
[3] S. Devaraj and N. Munichandraiah, Electrochem. Solid-State Lett., 8, A373 (2005).
[4] V. Khomenko, E. Raymundo-Pinero, and F. Beguin, J. Power Sources, 153, 183 (2006).
[5] P. Simon, Y. Gogotsi, Nat. Mater. 7, 845 (2008).
[6] S. C. Pang, M.A. Anderson, T.W. Chapman, J.Electrochem. Soc. 147, 444 (2000)
[7] J. Broughton, M. Brett, Electrochim. Acta 49, 4439 (2004)
[8] M.Cheong, I.Zhitomirsky, Surf. Eng. 25, 346 (2009)
[9] V. Augustyn, P. Simon, and B. Dunn, Energy Environ. Sci., 7, 1597 (2014)
[10] A. Balducci, J. Power Sources 326, 534 (2016)
[11] Y. Gogotsi, P. Simon, Science 334, 917 (2011).
[12] K.Shi, I.Zhitomirsky, J.Power Sources, 240, 42 (2013)
[13] M.S.Ata, R.Poon, A.M.Syed, J.Milne and I.Zhitomirsky, Carbon, 130, 584 (2018)
[14] M.S.Ata, Y.Liu, I.Zhitomirsky, RSC Adv. 4, 22716 (2014)
[15] Y.Yu, Q.Wang, J.Yuan, X.Fan, P.Wang and L.Cui, Carbohydrate Polymers 137, 549 (2016)
[16] A.Clifford, X.Pang and I.Zhitomirsky, Colloids Surfaces A, 544, 28 (2018)
[17] X. Ren, P.G. Pickup, J. Electroanal. Chem. 372, 289 (1994)
[18] J. Tanguy, N. Mermilliod, M. Hoclet, J. Electrochem. Soc. 134, 795 (1987).
[19] B.J. Feldman, P. Burgmayer, R.W. Murray, J. Am. Chem. Soc. 107, 872 (1985).
[20] Y.Wang, Y.Liu and I.Zhitomirsky, J. Mater. Chem.A, 1, 12519 (2013).
[21] J.Milne and I.Zhitomirsky, *J.Colloid. Interface Sci.,* **515**, 50 (2018)